Research Square

Preprints are preliminary reports that have not undergone peer review.
They should not be considered conclusive, used to inform clinical practice,
or referenced by the media as validated information.

Frequency and field-profile tuning of the ESS-Bilbao RFQ using a genetic optimization approach

Juan Luis Muñoz

jlmunoz@essbilbao.org

ESS Bilbao

Ibon Bustinduy

ESS Bilbao

Research Article

Keywords: RFQ, tuning, genetic optimization, accelerator control, surrogate models, machine learning

Posted Date: June 18th, 2026

DOI: https://doi.org/10.21203/rs.3.rs-9555850/v1

License: This work is licensed under a Creative Commons Attribution 4.0 International License.
Read Full License

Additional Declarations: No competing interests reported.

Frequency and field-profile tuning of the ESS-Bilbao RFQ using a genetic optimization approach

Juan Luis Muñoz[1*] and Ibon Bustinduy[1†]

[1*]Accelerator Division, ESS-Bilbao, Zamudio, Spain.

*Corresponding author(s). E-mail(s): jlmunoz@essbilbao.org;
Contributing authors: ibustinduy@essbilbao.org;
†These authors contributed equally to this work.

Abstract

The ESS-Bilbao radio-frequency quadrupole (RFQ) for the HiCANS platform has been tuned using a genetic optimization approach to achieve both the target resonant frequency and the required longitudinal field profile. Conventional bead-pull tuning methods based on the inversion of the linear response matrix were used as a first step, but their application was limited by the reduced actuator range of the plunger tuners and by the nonlinear behavior observed in the actual cavity. In this work, we present the tuning procedure applied to the 3 MeV, 352.2 MHz proton RFQ developed at ESS-Bilbao. The conventional approach is first introduced and its limitations described. A genetic algorithm is then used to search for tuner configurations that simultaneously satisfy mechanical tuner constraints and minimize field-profile errors. The combined strategy allowed the cavity to be tuned to the target operating frequency while significantly improving field flatness and reducing dipolar components. The results also illustrate the relevance of advanced numerical optimization methods as a first step toward AI-assisted surrogate models, reinforcement-learning control strategies and data-driven operation of future accelerator-based neutron source at ESS-Bilbao.

Keywords: RFQ, tuning, genetic optimization, accelerator control, surrogate models, machine learning

1 Introduction

The HiCANS Platform [1] will demonstrate the feasibility of a full high current accelerator driven neutron source in Europe. This platform will use the high current proton accelerator system (3 MeV) from ESS-Bilbao together with the target-moderator-reflector unit built and tested at JCNS [2] and the HERMES time-of-flight reflectometer instrument from LLB [3]. The proton accelerator consists of an ion source and a Low Energy Beam Transport (LEBT), which will inject the beam into an RFQ (Radio Frequency Quadrupole) linear accelerator. The RFQ will accelerate the 45 keV proton beam extracted from the source to the required 3 MeV.

The RFQ for the HiCANS Platform project at ESS-Bilbao is a linear accelerator that will accelerate the proton beam extracted from the ion source from 45 keV to 3.0 MeV. In general, an RFQ is a linear accelerator that takes as input the beam extracted from the ion source, bunches it to synchronize it with the radio-frequency (RF) field, keeps the beam focused, and accelerates it to the desired kinetic energy. The RFQ can perform these tasks because of the particular shape and magnitude of the electric field distribution inside the cavity. RFQ tuning, the main topic of this paper, involves not only setting up the correct resonant frequency of the cavity but also ensuring that the electric field has the required longitudinal profile. Since this tuning process depends on many coupled mechanical and electromagnetic parameters, it provides a suitable case study for the use of advanced numerical optimization methods.

Beyond the specific tuning of the ESS-Bilbao RFQ, this problem is representative of broader challenges in present and future accelerator research infrastructures, where many coupled subsystems, nonlinear responses, operational constraints and noisy diagnostics must be handled simultaneously. In this context, advanced numerical optimization, machine learning, Bayesian optimization and reinforcement learning are increasingly being considered to complement physics-based models in commissioning and operation. The genetic optimization approach presented here can therefore be regarded not only as a practical solution to the RFQ bead-pull tuning problem, but also as a first step toward more general data-driven and AI-assisted tuning strategies for the HiCANS platform and future ESS-Bilbao accelerator facilities like ARGITU [1].

1.1 Description of ESS-Bilbao RFQ

Physically, the RFQ is a copper structure of about 3.1 m long (Fig. 1). The operating frequency is 352.2 MHz (Table 1) [4], [5]), which should correspond to the the resonant frequency of the RFQ quadrupolar mode. In this quadrupolar mode, the standing RF wave has a particular spatial distribution of electric and magnetic fields. A brief description of this distribution is provided now because it is relevant for the described tuning procedure. In the absence of vane modulation, the electric field would have only transverse X and Y components (with Z being the beam propagation direction). The electric field distribution for the quadrupolar resonant mode is concentrated in the central inter-vane region, whereas the corresponding magnetic field, directed in the Z direction, has high absolute values in the external lobe regions while it is nearly zero in the central part (see 2). These transverse components of the electric field are responsible for the alternate beam focusing of the RFQ.

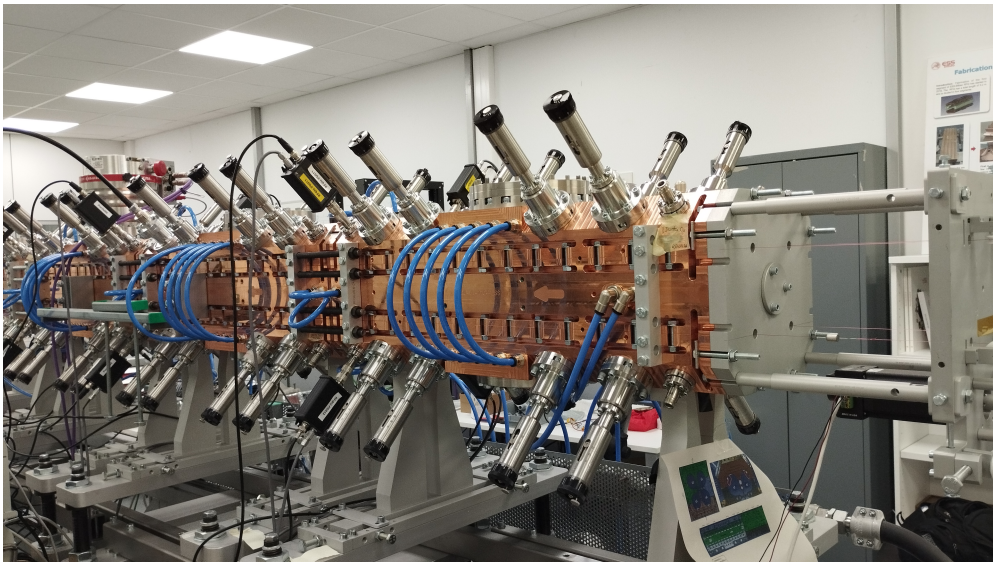


Fig. 1 A picture showing the RFQ in the bead-pull test bench. In the picture, the mechanical actuators for the plunger tuners and the power detectors for the pick-up coils can be seen. The bead-pull apparatus can be seen in the right hand part of the picture.

The bunching and accelerating characteristics of the RFQ need a longitudinal component of the electric field. This Z-directed component is created by the geometric modulation of the vane tips. The magnitude of the longitudinal electric field component is controlled by the amplitude of the geometrical modulation of the vane tips. This is small in the first section of the RFQ for gently bunching the beam, but is much bigger in the accelerator section of the RFQ (see 3). The wavelength of the modulation changes along the RFQ length, so the field generated is always synchronized with the RF frequency and the beam velocity.

The amplitude of the electric field in the inter-vane region has to be equivalent to the one that would be obtained if a stationary voltage (85 kV in our case) was applied to the vane tips. The electric field would then have the right focusing, bunching and accelerating characteristics so the RFQ can operate as intended, accelerating the beam from 45 keV to 3.0 MeV. This condition is referred to here as the "uniform voltage" case, in which the equivalent voltage along the RFQ length is constant, $V(z) = V_0 = 85\,\mathrm{kV}$. In reality, it is not possible to set the vane tips at a certain voltage; these field values will be reached when an adequate level of RF power which compensates the RF losses in the copper structure, is coupled to the RFQ cavity. In this case, the equivalent voltage will no longer be uniform, $V(z) \neq V_0$.

The vane modulation described above is itself a perturbation of the vane shapes. As the distance between the vane tips changes along the length, the capacitance of an equivalent LC circuit would change accordingly, so the transversal resonant structure no longer has the perfect quadrupolar field distribution shown in 2. The effect of the modulation is that the 3D resonant model can no longer be described by an intervane

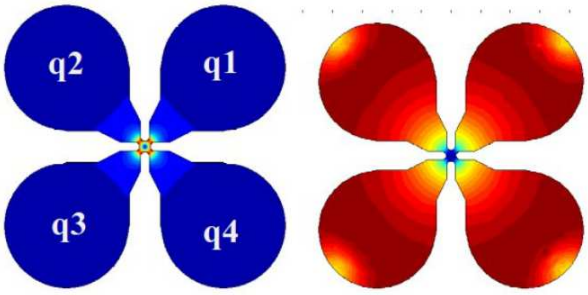


Fig. 2 Field distribution of the quadrupolar resonant mode of the RFQ cavity in cross-sectional view. The electric field (left) is concentrated in the central inter-vane region, whereas the magnetic field (right) is distributed in the external lobe regions. The quadrant numbering convention $(q_1, \ldots, q_4)$ is also shown.

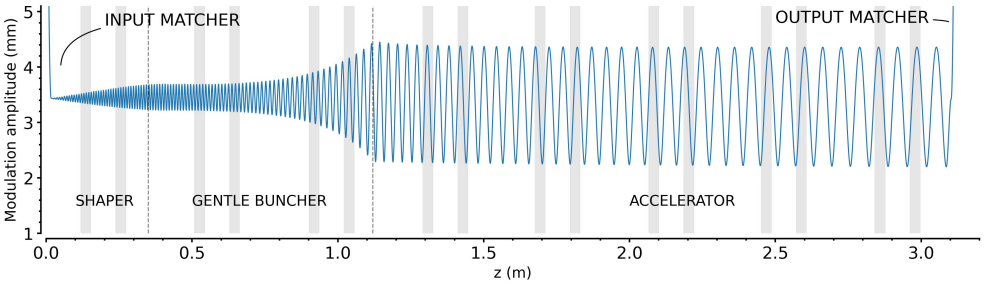


Fig. 3 Vane modulation curve for the RFQ. The curve represents the actual shape of the vane tips along the 3.1 meters length of the cavity. The different bunching and acceleration stages are also shown. The longitudinal positions where plunger tuners are located are shown as shaded bars in the picture.

voltage constant (85 kV in our case), but rather by a variable voltage or field amplitude $V = V(z)$. Additionally, the mechanical fabrication, machining, and assembly of the RFQ copper segments result in a cavity that is not perfectly identical to the design cavity. Any small difference will result in a deviation of the cross-section resonant perfect quadrupolar configuration, and this also appears as a perturbation on the field distribution along the longitudinal direction.

As a consequence of all these effects, the magnetic field components measured along the 4 lobes q1 to q4 (in Fig. 2) are not only non-uniform along the longitudinal dimension, but also will be different among themselves. This will also happen to the electric field components in the inter-vane region. The resulting accelerating field will then be different from the ideal designed one, and will also be asymmetrical for particles traveling along different XY quadrants, resulting in perturbations in the beam transfer and acceleration.

As described in previous references for this RFQ ([4], [5], [6], [7], [8]), a set of 62 plunger tuners can be inserted into the structure to locally modify the field equilibrium. The local perturbation will result in global (lengthwise) perturbation that can be used

Table 1 ESS-Bilbao RFQ main parameters.

Type	4 vane
Particle	Protons
RF frequency	352.2 MHz
Intervane design voltage	85 kV (uniform)
Energy	45 keV $\longrightarrow$ 3.0 MeV
Design current	60 mA
Input emittance (rms norm)	0.25 π mm mrad
Duty cycle	Up to 10%
Kilpatrick factor	1.85
Number of cells	273
R_0	3.44 mm
ρ/R_0	0.85
Input/output matcher	16.674 mm / 14 mm
Total length	3.12 m (3.66 λ)
Number of segments	4 (about 800 mm each)
Method of assembly	Polymeric vacuum gaskets
Plunger tuner ports	16 per segment

to compensate the modulation and fabrication perturbations, so the design voltage profile ($V(z) = V_0$ in our case, although non-uniform profiles are also common in other RFQs) can be recovered. Of course, the cavity frequency also changes as we modify the tuners. This procedure of inserting plunger tuners in the right way to set the frequency and the appropriate field profile is called the tuning of the RFQ.

2 Bead-pull tuning of an RFQ

As described in the previous section, the tuning of the RFQ refers to the procedure of using the set of plunger tuners to modify the field profile to achieve the desired one. The first step in this process is to actually measure the field profile in the RFQ cavity. This is realized by using the "bead-pull technique", where a small metallic element (the bead) is moved along the length of the RFQ in a high magnetic field region (external lobes close to cavity surface). The metallic bead locally perturbs the magnetic field, and this perturbation can be measured by a change of the phase of an RF signal detected by a network analyzer. The change in phase will be proportional to the local field, so measuring this change in phase with respect to the longitudinal position will be equivalent to measuring the magnetic field profile along the length of the RFQ. The magnetic field in the external lobe region will have the same profile as the electric field profile in the inter-vane region. Representative references on conventional RFQ bead-pull tuning techniques include the following Refs. [9–18].

From the measurement of the profile along the four quadrants q_1 to q_4, the derived magnitudes Q, D_s and D_t can be obtained as described in equation 1.

$$\begin{aligned} Q &= (q_1 - q_2 + q_3 - q_4)/4 \\ D_s &= (q_1 - q_3)/2 \\ D_t &= (q_2 - q_4)/2 \end{aligned} \tag{1}$$

In a perfectly tuned RFQ, $Q(z)$ will be equal to the design voltage profile ($Q(z) = V_0$), while the dipolar or asymmetric components D_s and D_t will be zero. The aim of the tuning procedure will be to approach this ideal situation as much as possible while maintaining a set of tuner penetrations that yields the correct cavity frequency.

Starting from a given set of tuner penetrations, the effect of moving one tuner by a certain distance, either inward or outward, changes the profiles Q, D_s and D_t for all values of z. This change can be computed using a transmission line analogy and a perturbation theory approach. It is assumed (see, for example, [19] for the conventional theory) that a first order perturbation that results in linear changes is in general enough for the cavity tuning requirements. This implies that only small changes in tuner penetration are considered. For a tuner placed at $z = z_0$ that when moved in or out of the cavity results in a frequency change $\Delta\omega_0$, the change in each of the field profiles can be described as in 2.

$$\frac{\delta V_0(z)}{V_0} = -8\frac{\delta\omega_0}{\omega_0}\left(\frac{l_v}{\lambda}\right)^2 \sum_{m=1}^{\infty} \frac{\cos\left(\frac{m\pi z_0}{l_v}\right)\cos\left(\frac{m\pi z}{l_v}\right)}{m^2} \tag{2}$$

In the first order approximation we can assume that the frequency change when a tuner is moved is independent of the tuner location in the RFQ. This means that $\delta\omega_0$ is proportional to $\Delta\overrightarrow{T}$, the same linear dependence for all the tuners. With this assumption, the change in field (or voltage) measured at a certain position $z = z_j$ when the tuner located at $z = z_i$ is modified by $\Delta T(z = z_i)$ can be written as [19]:

$$\Delta V(z = z_j) \;=\; m(z_i, z_j) \cdot \Delta T(z = z_i) \tag{3}$$

or, simply, $\Delta V_j \;=\; m(i,j)\Delta T_i$. The $m(i,j)$ values will be different for each of the derived magnitudes Q, D_s and D_t. Finally, considering only a subset of P z longitudinal positions and grouping the P measurements for Q, D_s and D_t in a $3P$ column vector, the above formula can be written in matrix form as:

$$\overrightarrow{V} = M \cdot \overrightarrow{T} \tag{4}$$

where $\overrightarrow{V}$ is a vector of length $3P$ containing the field-profile values at the P selected longitudinal positions, and $\overrightarrow{T}$ is a vector of length N containing the changes in the tuner penetrations. The response matrix M has dimensions $3P \times N$, with elements $m_{i,j} \;=\; \frac{\partial V_j}{\partial T_i}$. Due to the linear approach used, the elements of the M matrix will be obtained from bead-pull measurements of the RFQ as described in the next section.

2.1 Setting M matrix values from measurements

The actual profiles $Q(z)$, $D_s(z)$ and $D_t(z)$ are measured using the bead-pull technique. Selecting the P longitudinal measurements at certain z coordinates, a set of vectors $\overrightarrow{V}$ is obtained. Starting from a defined initial configuration (for example, with all tuners with the same penetration), the procedure to obtain the M matrix is described in the algorithm 1. Each measurement corresponds to a complete set of 4 longitudinal bead-pull runs for each of the quadrants $q1$ to $q4$. The signals measured (actually a phase change in the S_{21} RF measurement) are pre-processed to shift all traces to the

same starting coordinate and zero level. From the four traces $Q1$ to $Q4$, the derived magnitudes Q, D_s and D_t are computed as in Eq. 1. Finally, P discrete coordinates are selected from the traces. These coordinates will then be used for all the measurements and subsequent analysis. The 3 vectors of length P are arranged in a common vector $V = \{Q, D_s, D_t\}$ of length $3P$ that summarizes a single measurement of the RFQ.

Algorithm 1 Setting up matrix M from bead-pull measurements

Require: Set initial tuner configuration of the N tuners, $T = T_0$.

1: Set empty M matrix with N columns and $3P$ rows
2: Select P positions along the RFQ length
3: Measure field profile and build base vector $V_0 = \{Q_0, D_{s0}, D_{t0}\}$
4: Select a unit change of the tuners, δ_t (i.e. a penetration of +5 mm)
5: **for** $j = 1$ to N **do**
6: Set tuner configuration T_0
7: Move tuner j a distance δ_t, $T_j = T_j + \delta_t$
8: Measure field at 4 quadrants and get $V_j = \{Q_j, D_{sj}, D_{tj}\}$
9: $\delta V_j \Leftarrow V_j$ - V_0
10: Matrix M column $j \Leftarrow \delta V_j$ / δ_t
11: **end for**

In this way, matrix M represents a linear relationship between the action of the tuners and the changes in the field profile. As mentioned above, this approach assumes that the changes are small and can be represented by a linear function.

The matrix M relates the changes in the tuner penetration to changes in the field profile: $\Delta V = M \cdot \Delta T$. The tuning of the RFQ then requires the inverse operation: finding the changes in tuner penetration, $\Delta\overrightarrow{T}$ that produce the desired field change, $\Delta\overrightarrow{V}$. In our case, this means that the components of the vector $V = \{Q, D_s, D_t\}$ are $Q = \{V0, ...V0\}$ and D_s and D_t are equal to zero. The values of these vectors are normalized with respect to V_0, as the aim is to obtain a uniform profile.

Mathematically, this requires inverting the matrix M, so we can get $\Delta T = M^{-1} \cdot \Delta V$, where $\Delta\overrightarrow{V}$ is the desired field change.

2.2 Conventional SVD algorithm for matrix inversion

Since matrix M is generally not square, it is not possible to obtain directly the inverse matrix M^{-1}. Instead, the pseudoinverse matrix obtained by application of the SVD algorithm (Singular Value Decomposition) is used (see, for example, [14]). In this approach, the matrix M, of size $(3P \times N)$, is decomposed as $M = U \cdot S \cdot V^T$, where U and $\overrightarrow{V}$ are square matrices, and S is a diagonal matrix whose elements are the singular values of the matrix M: $S = \text{diag}\{\sigma_1, \sigma_2, \ldots\}$. This apparently complicated procedure is very useful because the pseudoinverse matrix M^{-1} can then be calculated as: $M^{-1} = V \cdot S^{-1} \cdot U^T$, where the matrices U and $\overrightarrow{V}$ are already computed, and $S^{-1} = diag\{1/\sigma_1, 1/\sigma_2, ...\}$.

From the pseudoinverse matrix obtained this way, it is possible to directly compute the optimum tuner change that will result in the desired voltage or field profile vector $Q = \{Q, D_s, D_t\}$:

$$\Delta T \;=\; M^{-1}\,\Delta Q \;=\; (\,V\,S^{-1}\,U^{T})\Delta Q \tag{5}$$

A commonly found problem in this approach is that the values of the $\Delta\overrightarrow{T}$ vector obtained this way are not constrained in any way. As a result, the proposed values of the tuner displacements can include movements that are outside the actual tuner movement range. To try to overcome this situation, the following iterative procedure is used. The matrix S is a diagonal matrix. The elements of this matrix are sequentially set to zero: in the iteration step j, the diagonal element $N-j$ is set to zero. Then each step matrix S has more elements set to zero than the previous one, so the proposed tuner configuration for each of these steps, $\Delta T^{(j)} \;=\; (\,V\,{S_j}^{-1}\,U^{T})\Delta Q$ is smaller than the previous step. This can result in a proposed tuner change that can be physically attainable, but at the same time the result will deviate from the ideal flat voltage profile that would be obtained with the exact solution that uses the whole S matrix. This procedure continues iteratively, setting more elements of the S matrix to zero until a good enough tuner configuration is selected.

The proposed tuner configuration is then implemented in the RFQ cavity by moving all the tuners to the prescribed positions. Then the field profile is measured again by the bead-pull technique and, if the measured result is still not as good as required, a new SVD iterative procedure is carried out.

2.2.1 ESS-Bilbao RFQ initial configuration and SVD algorithm application

For the ESS-Bilbao RFQ, after assembly and setup of the bead-pull equipment, a starting tuner configuration was established. In this initial configuration, all tuners were inserted to the same penetration, $\delta = 10\,\text{mm}$. In the RFQ, there are 62 tuners inserted (16 per segment times 4 segments, minus two ports that are used for the power couplers).

With this uniform penetration, the RFQ frequency is measured to be 349.995 MHz. The profile of the fields for the four quadrants, and the corresponding derived magnitudes in this initial state, are shown in Fig. 4. The upper plot shows the traces for the four B_1, B_2, B_3, B_4 quadrants, while in the lower plot the derived magnitudes Q, D_s, D_t, defined in Eq. 1 and normalized to an average $Q = 100$ are shown. It is clear that the field profiles are far from flat. The Q-curve shows the expected profile that can be computed with the transmission line model taking into account only the modulation itself, while the D_s and D_t traces, that reflect asymmetries in the assembly or fabrication of the RFQ components, are quite above the desired deviation of 2% around the optimum set of $\{Q, D_s, D_t\} = \{100, 0, 0\}$ fields. The range of variation of the Q curve is between 75% and 125%.

In the lower panel of Fig. 4, the red crosses mark the points selected to build the Q vector of measurements. There are 19 points in each trace, so the Q vector will be a vector of length 57. From this initial or base configuration, the matrix M is measured as described in the previous section. Each tuner is inserted $+5\,\text{mm}$ in sequence, the bead

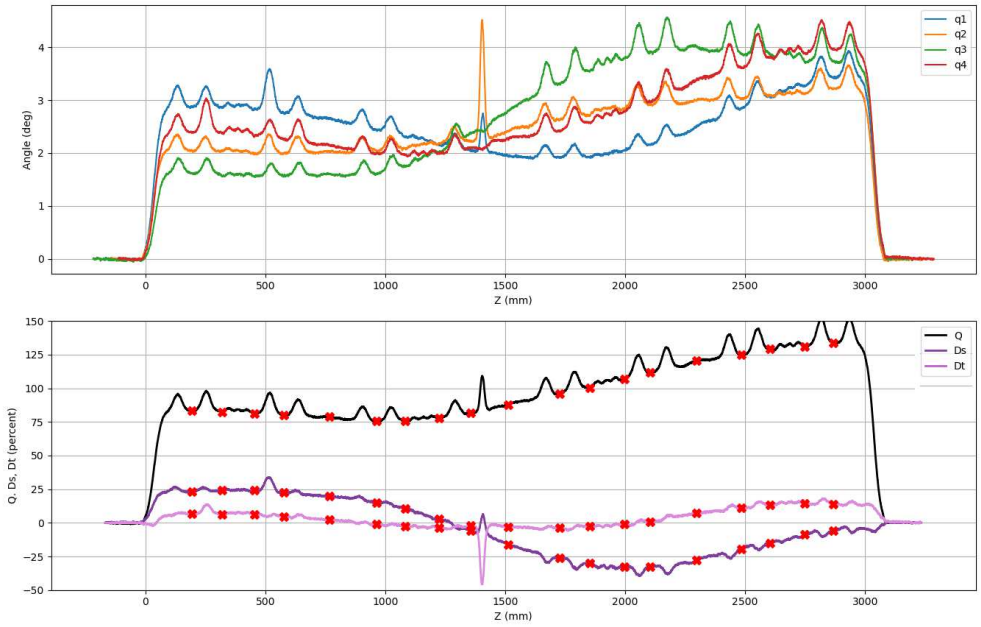


Fig. 4 Field profile traces measured along the ESS-Bilbao RFQ length. The upper panel shows the magnetic field profiles B_1, B_2, B_3, B_4 measured in the four quadrants (q_1 to q_4). The lower panel shows the derived and normalized quantities $\{Q, D_s, D_t\}$. The crosses indicate the discrete points selected for the tuning procedure.

pull traces are collected, and the derived $\{Q, D_s, D_t\}$ are computed and normalized. The 57 selected values are then arranged in a vector Q, and a vector ΔQ is computed as the difference from the initial configuration. If the tuner number i was acted upon, then the measurement of the Q vector represents the i-th column of the M matrix. The matrix M is filled this way. A representation of the matrix is shown in Fig. 5.

The outcome of the SVD sequence is shown in Fig. 6. The initial base situation is the measured field profile when all tuners are inserted with a uniform penetration of 10 mm. The direct result of the algorithm corresponds to the first step number in the plots. The predicted values for $\{Q - 100, D_s, D_t\}$ are quite good (close to zero), but the required tuner displacements that the model suggests to achieve them are outside of the actual physical extent of the tuner actuators (in Fig. 6 only the maximum and minimum of the 62 suggested tuner changes are plotted). As described above, setting values of the S matrix to zero iteratively we obtain proposed solutions that suggest smaller tuner movements, but at a price of resulting in worse field profile outcomes. For our RFQ, the first possible set of changes of tuner penetrations that we could realize was the one for step number 11, with tuner variations within -15 mm (outward) and +10 mm (inward) range. For this step, the predicted result is not perfect but good enough (average error around 2%) for a first iteration of the whole process.

The proposed tuner configuration was then realized in the RFQ cavity (changing the penetration of the 62 tuner actuators) and the field profiles were measured again.

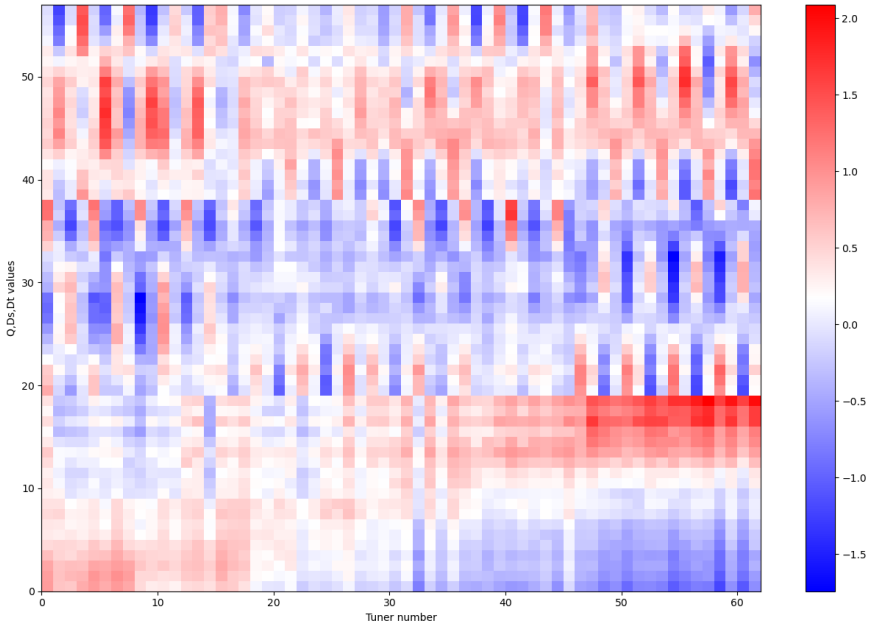


Fig. 5 Graphical representation of the M matrix for the ESS-Bilbao RFQ. The color range represents $M_{ij} = \partial Q_i / \partial T_j$.

The result represented an important improvement of the field profiles, but was far from the magnitudes predicted by the inversion matrix algorithm. These results indicate that the assumption of small linear changes is not fully valid. As the problem is not linear, several steps taking the previous result as the next starting point are needed until the procedure converges to a solution.

This procedure has been carried out with the RFQ, and after several iterations, a situation like the one depicted in Fig. 7 was achieved. It is clear that these profiles are much flatter than the starting ones shown in Fig. 4. The errors in the averages of $\{Q - 100, D_s, D_t\}$ are close to 4%. The frequency of the quadrupolar mode of the RFQ cavity at this step is 350.192 MHz. The proposed tuner variations from the initial situation have an average value close to zero, so the overall change in cavity frequency should also be small.

2.2.2 Limits of the SVD approach

The tuning of the RFQ proceeds in an iterative way. After measuring the field profiles, the magnitudes of the vector $Q = \{Q, D_s, D_t\}$ are collected and the tuner changes are computed using the matrix inversion approach, $\Delta T = M^{-1}(Q - Q_0)$, using the pseudoinverse coming from the SVD algorithm. Then the tuners are moved as proposed by the result of the model ($T_i = T_i + \Delta T_i$), the fields are measured again by the bead-pull technique, and the procedure starts again until a good enough field profile is obtained. Between any of these steps, the tuner penetrations can be incremented

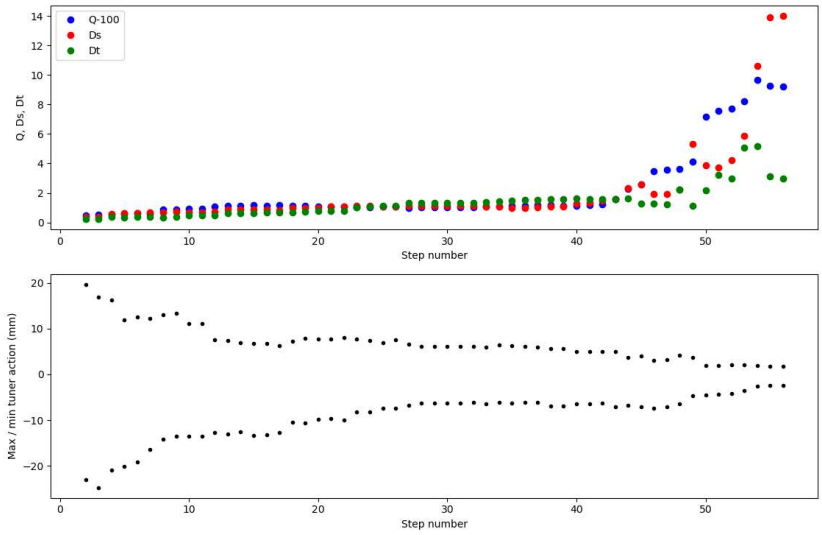


Fig. 6 Outcome of the SVD algorithm starting from a uniform tuner penetration of 10 mm. The x-axis represents the iterations in the algorithm (see text for details). In the upper panel the predicted average values for vectors $\{Q, D_s, D_t\}$ are shown. In the lower panel the maximum and minimum tuner-penetration changes proposed by the model are presented.

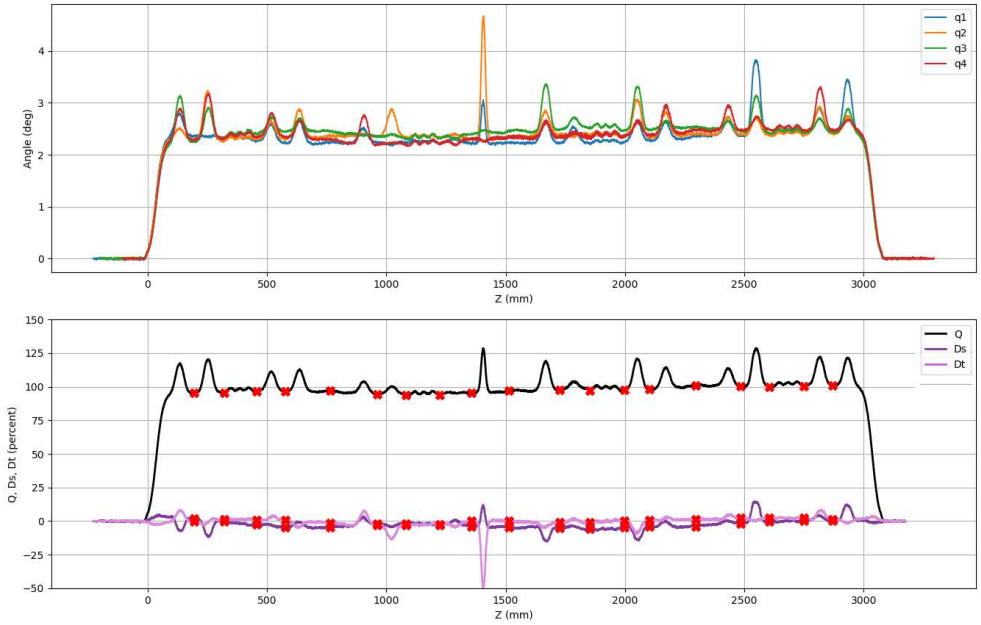


Fig. 7 Measurement of RFQ field profiles after the last SVD algorithm step. The magnitudes plotted are the same as in Fig. 4. The profiles deviations from the ideal case are about 4%.

(uniformly for all tuners) a certain amount to increase the cavity frequency towards the target one.

From the RFQ situation described in Fig. 7, it was not possible for us to continue refining the field profiles and increasing the cavity frequency assisted by the SVD algorithm. The proposed sets of tuner displacements contained always values outside of what is possible to achieve with our tuner actuators or other physical constrain, like possible collisions with the bead for the bead-pull. Furthermore, to increase the cavity frequency we required to insert the tuners close to the their maximum range and out of the linear frequency dependence.

Additionally, the set of measurement points selected to populate the vector Q (red crosses in Figs. 4 or 7) was selected before the procedure started because these positions are required to build up the response matrix M. The positions are selected to avoid the deformation of the curves caused by the bead moving too close to the tuners or the coupler loops as they move inside the RFQ cavity. When the tuner penetrations are high, as was the case for frequencies close to the operational one, these deformations or bumpings of the curves are more noticeable and affect the field measurements and the overall procedure.

2.3 Genetic algorithm tuning

To overcome some of the above difficulties and to proceed with the RFQ tuning in field profile and cavity frequency, a procedure based on a genetic optimization algorithm was designed. The procedure was previously tested with FEM simulations of the RFQ [8] and has been used for the actual tuning of the RFQ and is reported here for the first time. The use of this alternative approach was motivated by the fact that the conventional SVD approach could not be used to improve the ESS-Bilbao RFQ tuning beyond what has been discussed in the previous section. The genetic algorithm resulted in a reliable approach to adjust the RFQ by finding tuner configurations that are compatible with the actual possible tuner displacement. As far as the authors know, this is the first report of such an application to an actual RFQ cavity.

The genetic algorithm takes advantage of the response matrix M built from bead-pull measurements of unit changes of the tuner penetration. As described above, the matrix M relates any change in the tuner penetrations from a particular configuration to the change in the field values along the RFQ $\Delta Q = M \cdot \Delta T$. Instead of inverting the matrix M to obtain the tuner change ΔT_0 that will produce the desired change in field profiles ΔQ, it is possible to use the direct formulation and an optimization algorithm to find the optimum tuner change.

In the optimization algorithm, the aim is to find an optimal vector of tuner-penetration changes that would result in the best possible evaluation (values of $Q = \{Q, D_s, D_t\}$) close to $\{100, 0, 0\}$). In the genetic algorithm language, each vector of tuner-penetration changes, $\overrightarrow{T}$, is treated as an individual x in a larger population. The values of vector $x = (x_0, x_1, ...x_{62})$ are discretized to a certain number of significant digits and written in a numeric sequence that represents its genetic code. The fitness of each individual x in the population is evaluated using a fitness function that computes the predicted field profile from it using the linear matrix M and returns a certain fitness value. Individuals with high fitness values are propagated to the next

generation, possibly with small changes or mutations, whereas individuals with low fitness values are discarded. Following this approach, the population of possible tuner changes will be more and more populated with solutions closer to the desired one, until the procedure converges to an optimum one.

This approach also uses the approximated linear system represented by matrix M, so several iterations of the whole procedure (computing solutions, setting them up in the RFQ and measuring the result, which will be the next starting point) are required until convergence of the RFQ tuning is achieved.

This procedure makes it possible to control the range of tuner configurations explored by the algorithm. For example, it is possible to choose the possible tuner displacement from a fixed range, in order to ensure that the obtained solution can be physically set up with the tuner actuators. If a proposed individual contains tuner values outside the range, the fitness function adds a penalty that prevents it from being propagated as the algorithm progresses.

In the particular interpretation used for ESS-Bilbao RFQ, implemented using the PyGAD library [20], an initial population of $N = 500$ individuals is randomly created. Each individual x is then a vector that represents a displacement of the 62 mechanical tuners (number of genes). The fitness function evaluation computes the predicted outcome of this tuner change, $Q(x) = Q_0 + M \cdot x$. The result $Q(x)$ will be the vector containing the field profiles, as described above. From this vector a derived fitness value is computed comparing the profile outcome with the target one and getting an rms error, y. This ensures that the predicted RFQ field profile deviation from the ideal one is, on average, close to zero. This error is then augmented by different penalty functions, as shown in Algorithm 2. First, even if each individual tuner is inside the allowed movement range, a soft range penalty (for example, around 2 mm change) is imposed. From each generation, the best individuals are selected using a steady-state selection procedure as well as a two-point crossover approach. A random mutation rate of 15% is applied to the resulting individuals.

This procedure runs quite fast on any computer, as it implies only evaluations of the direct matrix M system coupled with the evaluation of the fitness function. An example of the convergence function is shown in Fig. 8. The convergence is reached in about 350 generations for all the cases considered. This takes about 1 minute of run time on a regular laptop computer.

The converged solution is then a proposal of tuner changes that matches the specified criteria for tuner displacements while at the same time minimizes the error, so that the resulting field profiles are also optimized. This procedure has been carried out with the ESS-Bilbao RFQ in several steps, including steps to increase the cavity frequency. After some steps, the field profile shown in Fig. 9 is achieved. The genetic algorithm has been able to select a suitable tuner configuration during each of the steps, even when the frequency increase required to insert the tuners to values close to their maximum range. The final cavity frequency was set to 352.1 MHz, 100 kHz below the nominal operating RF frequency, to account for the expected frequency shift between measurements at atmospheric pressure and operation under vacuum.

The evolution of the whole tuning procedure, including the initial SVD steps and the following genetic tuning steps (configurations identified with a letter G) are shown

Algorithm 2 Fitness evaluation for a candidate tuner configuration

Require: Candidate tuner displacement vector $x = \{x_1, \ldots, x_N\}$
Require: Target profile Q_0
Require: Hard displacement bounds $[x_{\min}, x_{\max}]$
Require: Soft displacement bounds $[x_a, x_b]$
Require: Reference tuner positions $\{x_1^0, \ldots, x_N^0\}$
if $\exists i \in \{1, \ldots, N\}$ such that $x_i \notin [x_{\min}, x_{\max}]$ **then**
    return -10
end if
$Q_x \leftarrow Q_0 + Mx$
$q \leftarrow \mathrm{rms}(Q_x - Q_0)$
$penalty \leftarrow 0$
for $i = 1$ to N **do**
    if $x_i < x_a$ **then**
        $penalty \leftarrow penalty + (x_a - x_i)^2$
    end if
    if $x_i > x_b$ **then**
        $penalty \leftarrow penalty + (x_i - x_b)^2$
    end if
    if $x_i + x_i^0 \notin [0, 23]$ **then**
        $penalty \leftarrow penalty + 50$
    end if
end for
$y \leftarrow \dfrac{1}{q + penalty}$
$y \leftarrow \mathrm{sigmoid}(y)$
return y

in Fig. 10. The plot includes steps for field profile tuning and for frequency change. The tuning magnitudes are relative to a 100% magnitude of Q. The standard deviations of Q, D_s and D_t, as well as the average magnitudes of D_s and D_t are shown. As the objective of the tuning with respect to the field profile is, in our case, to obtain a flat profile (uniform voltage or field profile), the average value of the Q magnitude is not relevant, as it will represent the power injected into the cavity. The uniformity of the field along the length of the RFQ is better described by the standard deviation of Q. The frequency of the cavity is also shown for all steps. The cavity frequency has been increased up to the target value of 352.1 MHz.

2.4 Outlook on data-driven tuning approaches

The optimization procedure described above assumes a linear relationship between tuner displacement and field profile changes. This implies that the response matrix M, which is constructed from measurements and is the base for all the tuning methods used here, is a numeric matrix. The experimental data shows that the measured

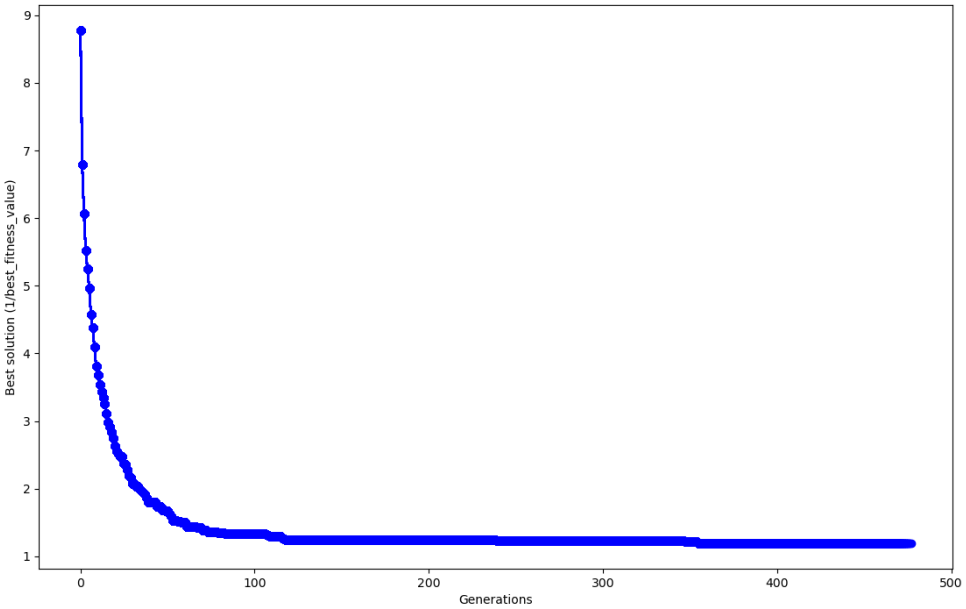


Fig. 8 Convergence of the genetic algorithm starting from an initial tuner configuration and measured field profiles. The algorithm finds an optimum solution in about 350 generations, corresponding to less than one minute of runtime on a regular laptop.

behavior deviates from this linear approximation, mainly because for high tuner penetration the perturbation on the magnetic field measurements (see for example the bumps in Fig. 9). To overcome this problem, several iterations are needed until a correct solution is found.

A nonlinear model can be implemented using an artificial neural network trained with measured data. This model would incorporate the nonlinearities of the measurement and could be used to better drive the tuning procedure. A problem for this approach is the small number of points in the data set. The model should have an input dimension $dim(X) = 62$ (vector of the 62 tuner changes) and an output dimension of $dim(Y) = 45$ (if 15 discrete measurement points are selected in the traces). To train the model we only have the 62 measurements of the base configurations (the ones used to create the M matrix, with single tuner variations) and about 30 additional measurements taken during the tuning procedure, with variations of all the tuners. This dataset is clearly insufficient to train a usable model. In any case, such a model would not be used to further tune the RFQ, as it will be moved to conditioning and operation phases and no further tuning is required. These base measurements were also recorded using small single tuner variations and for the initial situation where the RFQ cavity frequency was low (as described above). The nonlinearities are more noticeable for higher RFQ frequencies (closer to the operational one), that require larger tuner penetrations.

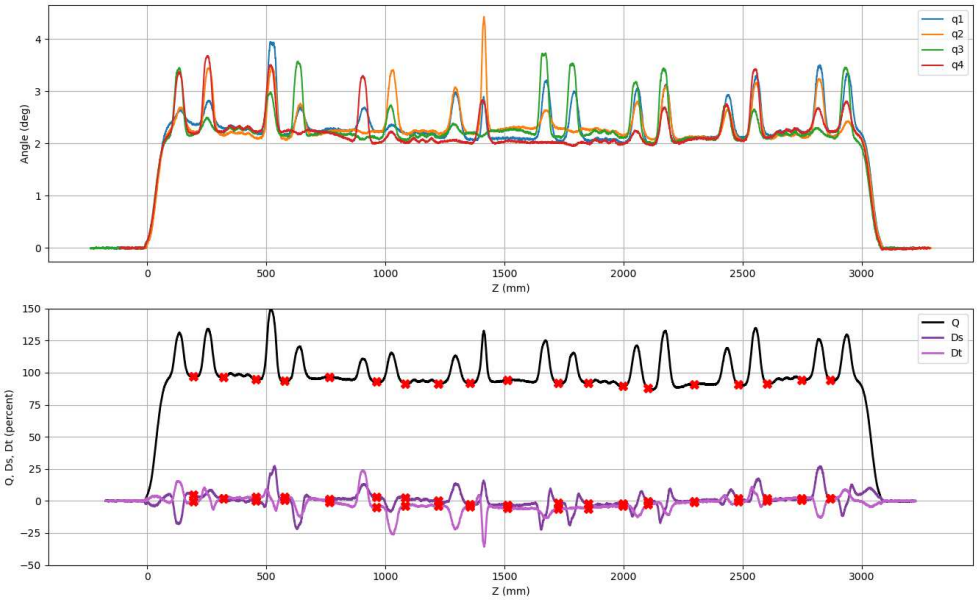


Fig. 9 Measurement of RFQ field profiles after application of the genetic algorithm for tuning. The cavity frequency has been increased to the target value of 352.1 MHz. The magnitudes plotted are the same as in Fig. 4.

In order to have a model that could reflect the changes in the field profile during high power conditioning and during beam operation, the measurements collected by the pick-up coils, placed along the RFQ length, could reproduce the field profile as measured by the bead-pull technique. The field profile variations in this case will not be caused by tuners displacement, but by thermo-mechanical deformation of the RFQ, and changes in power input by beam loading, etc. In order to better understand this and to have a tool to assist the operations, a model trained with simulation data can be generated. Such a model would require a finite-element simulation framework capable of generating a large number of random configurations of tuners and power input and cooling conditions in the RFQ. The derived magnitudes (field profiles and frequency detuning) could be computed and a large dataset built automatically from the simulation data. This will be the topic of future work.

3 Perspective for AI and advanced numerical techniques in ESS-Bilbao

The tuning strategy presented in this work is also part of a broader trend in accelerator research infrastructures (RIs), where advanced numerical optimization and artificial-intelligence methods are increasingly being introduced to complement physics-based models. The HiCANS facility under development at ESS-Bilbao, as well as the future ARGITU accelerator-driven neutron source, share with other modern accelerators a

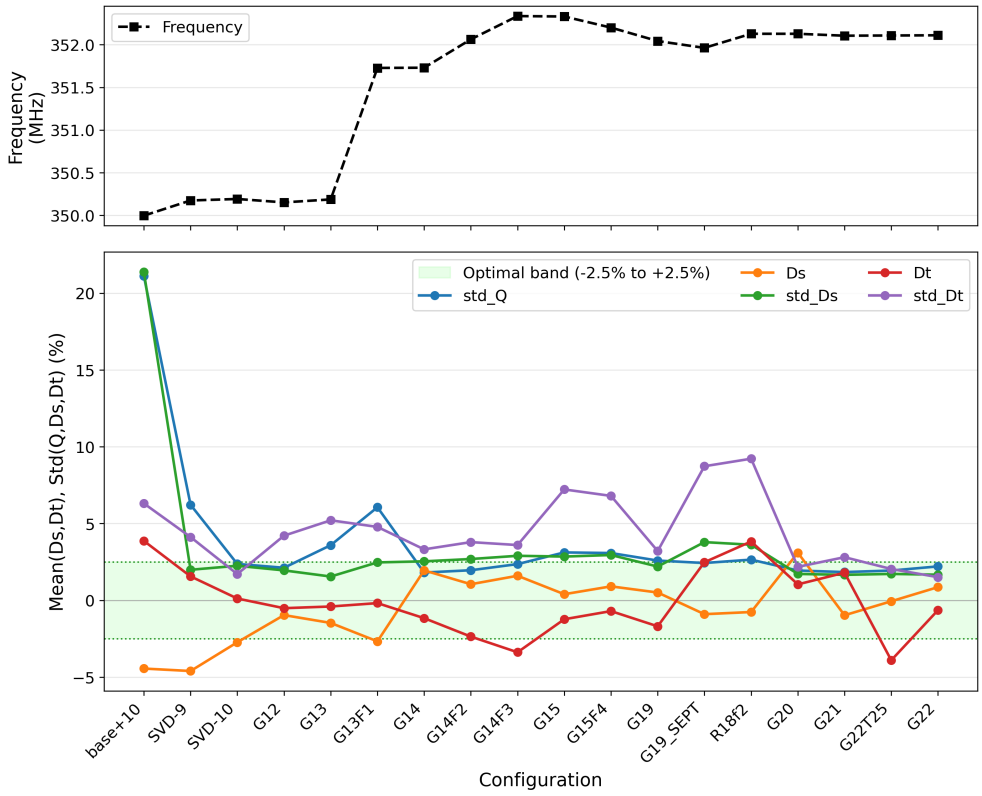


Fig. 10 Evolution of the tuning procedure for the ESS-Bilbao RFQ. In the upper plot, the resonant frequency for each configuration is shown. In the lower plot, the tuning magnitudes scaled to an average value of Q equal to 100% are shown. The standard deviation of Q, D_s and D_t, as well as the average magnitudes of D_s and D_t are shown. In the ideally tuned RFQ, these magnitudes would be equal to 0. The cavity frequency has been gradually increased up to the target value of 352.1 MHz. The error magnitudes are around 2% for the final configuration.

number of challenging features: many coupled subsystems, nonlinear responses, slow or noisy measurements, and operating conditions that may evolve dynamically and not always in a fully controlled manner. Examples include RF power trips, thermal drifts, variations in beam transport conditions, or other issues related to neutron-source operation. In this context, machine learning (ML), Bayesian optimization and reinforcement learning (RL) are being explored as tools to build surrogate models of the machine, assist beam-line tuning, and predict or anticipate alarm interlocks before they occur.

Within the immediate plans at ESS-Bilbao for the use of these technologies, the development of a surrogate model of the RFQ linac is a clear objective for HiCANS-platform operation. A first application of this concept has already been discussed in the previous section in relation to the RFQ tuning algorithm. A machine-learning approach, based on experimental data from the bead-pull tuning of the RFQ together

with finite-element simulations of the device, will be developed to provide a model suitable for use in the control room. Such a model could help interpret the measurements from the pick-up coils and suggest corrections to the power levels applied to the RFQ segments.

An additional surrogate model will be needed to address the thermo-mechanical detuning of the RFQ. As mentioned above, the average power during the first stages of HiCANS-platform operation is limited to a low duty cycle of 1%, and the cooling skid has been dimensioned accordingly. The RFQ linac is highly sensitive to changes in thermal conditions, since thermal expansion of the copper vane tips can produce significant shifts in the cavity frequency. In order to keep this frequency within the operational range, the cooling-water temperature and the input power level must be dynamically adjusted. This is a particularly suitable scenario for the implementation of an RL approach, in which an agent reads sensor measurements, such as reflected power, detuning and water outlet temperature, and learns to control the relevant operational parameters in order to keep the RFQ in tune.

A similar RL-based approach could also be applied to the transfer line of the HiCANS platform. In this section of the accelerator, 15 quadrupole magnets, together with their associated vertical and horizontal corrector magnets, can be adjusted to keep the beam at the required position and envelope, as measured by the appropriate diagnostics before entering the target station. The control of ion-source plasma conditions is another promising area in which to test these tools. In particular, a Bayesian optimization tool for the dynamic control of the magnetic field in the plasma chamber is already under development at the ESS-Bilbao proton injector for the HiCANS platform.

Many of these approaches are not unique to ESS-Bilbao, but rather reflect a shared interest among accelerator facilities worldwide. The existence of collaborative networks and a growing body of common knowledge in AI-assisted accelerator operation will allow the accelerator community to implement such improvements in a more reliable way, while facilitating training, reproducibility and the harmonization of tools and control-system methodologies.

4 Conclusion

A novel genetic-optimization approach was succesfully used to tune the ESS-Bilbao RFQ in frequency and field profile. The genetic algorithm made it possible to overcome the difficulties that the conventional procedure found due to the small tuner range that the tuner actuators have available. The procedure has resulted in an RFQ linac completely tuned and ready for high-power conditioning and operation.

Acknowledgements. The authors gratefully acknowledge the contributions of the ESS-Bilbao team to the bead-pull setup and RFQ preparation. In particular, the authors thank N. Garmendia, P. Gonzalez, A. Conde and J. Martin for their work on the bead-pull setup and RF measurements, and D. Fernandez-Canoto, G. Harper and S. Masa for their contributions to the RFQ cooling setup.

References

[1] Pérez, M., Sordo, F., Bustinduy, I., Muñoz, J.L., Villacorta, F.J.: Argitu compact accelerator neutron source: A unique infrastructure fostering r&d ecosystem in euskadi. Neutron News **31**(2-4), 19–25 (2020) https://doi.org/10.1080/10448632.2020.1819140 https://doi.org/10.1080/10448632.2020.1819140

[2] Baggemann, J., Gutberlet, T., Zakalek, P., Wolters, J., Rücker, U., Mauerhofer, E., Li, J., Ding, Q., Loewenhoff, T., Dorow-Gerspach, D., Bessler, Y., Brückel, T.: High power target for the high brilliance neutron source. Nuclear Instruments and Methods in Physics Research Section A: Accelerators, Spectrometers, Detectors and Associated Equipment **1069**, 169912 (2024) https://doi.org/10.1016/j.nima.2024.169912

[3] Paulin, Mariano Andrés, Pechenizkiy, Ivan, Zakalek, Paul, Lieutenant, Klaus, Kämmerling, Peter, Steffens, Alexander, Kleines, Harald, Rücker, Ulrich, Gutberlet, Thomas, Gautrot, Sébastien, Menelle, Alain, Ott, Frédéric: The hermes reflectometer at the julic neutron platform. EPJ Web Conf. **286**, 03003 (2023) https://doi.org/10.1051/epjconf/202328603003

[4] Muñoz, J.L., Bustinduy, I., Igor, R., Cos, D.: Development of the radio frequency quadrupole proton linac for ess-bilbao DAES. EPJ Web of Conferences 231, 02001 (2020) **231**(02001), 173–196 (2020) https://doi.org/10.1051/epjconf/202023102001

[5] Bustinduy, I., Muñoz, J.L. (eds.): ESS-Bilbao RFQ Technical Design Report DAES. ess-bilbao, Zamudio (2015). Available online: https://www.essbilbao.org/st_docs/technical-design-report-ess-bilbao-rfq

[6] Garmendia, N., Muñoz, J.L., Bustinduy, I., González, P., Kaftoosian, A., Martin, J., Conde, A., Ángel, R., Masa, S.: Status and RF developments of ESS-Bilbao RFQ. LINAC2022, Liverpool, UK (TUPOPA03) (2022). https://doi.org/10.18429/JACoW-LINAC2022-TUPOPA03

[7] Muñoz, J.L., Bustinduy, I., Garmendia, N., Martin, J., Fernández-Cañoto, D., Pedro, G., Conde, A., Zugazaga, A., Kaftoosian, A.: Update on ESS-Bilbao RFQ LINAC. LINAC2024, Chicago, IL, USA. (MOPB034) (2024). https://doi.org/10.18429/JACoW-LINAC2024-MOPB034

[8] Muñoz, J.L., Bustinduy, I., Conde, A., Garmendia, N., González, P.J., Martin, J., Toyos, V.: ESS-Bilbao RFQ Static Tuning Algorithm and Simulation. JACoW Publishing, Geneva, Switzerland (2024). https://doi.org/10.18429/JACoW-HB2023-THBP03 . https://jacow.org/hb2023/papers/thbp03.pdf

[9] Berrutti, P., Khabiboulline, T.N., Poloubotko, V., Romanov, G., Steimel, J., Yakovlev, V., Li, D., Staples, J.: Pxie rfq bead pull measurements. In: Proceedings of LINAC2014, pp. 535–537. JACoW, Geneva, Switzerland, ??? (2014).

https://proceedings.jacow.org/LINAC2014/papers/tupp047.pdf

[10] Promdee, W., Boorman, G.E., Edgecock, T.R., Letchford, A.P., Pozimski, J.K.: Bead pull measurements of the fets rfq at ral. In: Proc. 8th International Particle Accelerator Conference (IPAC'17), pp. 4349–4351. JACoW, Geneva, Switzerland, ??? (2017). https://doi.org/10.18429/JACoW-IPAC2017-THPIK108 . http://jacow.org/ipac2017/papers/thpik108.pdf

[11] Akkurt, N., Algin, E., Unel, N.G.: Measuring the electromagnetic properties of radio-frequency quadrupole with bead-pull measurement technique. AIP Conference Proceedings **2042**(1), 020061 (2018) https://doi.org/10.1063/1.5078933

[12] Koubek, B., Grudiev, A., Timmins, M.: rf measurements and tuning of the 750 mhz radio frequency quadrupole. Physical Review Accelerators and Beams **20**(8), 080102 (2017) https://doi.org/10.1103/PhysRevAccelBeams.20.080102

[13] Xing, Q.Z., Yu, X.D., Guo, Q.K., Ma, P.F., Lei, Y., Zheng, S.X., Li, Y., Wang, S., Liu, K., Guan, X.L., Wang, X.W., Wang, B.C., Zhao, C., Wang, Z.M.: Field tuning and rf measurements of the four-vane radio frequency quadrupole with ramped inter-vane voltage. Physical Review Accelerators and Beams **22**(2), 020102 (2019) https://doi.org/10.1103/PhysRevAccelBeams.22.020102

[14] Pommerenke, H.W., Rienen, U., Grudiev, A.: rf measurements and tuning of the 1-m-long 750 mhz radio-frequency quadrupole for artwork analysis. Nuclear Instruments and Methods in Physics Research Section A: Accelerators, Spectrometers, Detectors and Associated Equipment **1011**, 165564 (2021) https://doi.org/10.1016/j.nima.2021.165564

[15] Marchi, M., Grudiev, A., Mathot, S., Pommerenke, H.: Rf measurements and tuning of the cern 750 mhz elisa-rfq for public exhibition. In: Proceedings of LINAC2022. JACoW, Geneva, Switzerland, ??? (2022). https://doi.org/10.18429/JACoW-LINAC2022-TUPOPA09 . https://doi.org/10.18429/JACoW-LINAC2022-TUPOPA09

[16] Piquet, O., Desmons, M., France, A.C., Delferriere, O.: Rf design of ess rfq. In: Proc. IPAC'12, pp. 3800–3802. JACoW, New Orleans, LA, USA (2012). https://doi.org/10.18429/JACoW-IPAC2012-THPPP031 . https://proceedings.jacow.org/IPAC2012/papers/thppp031.pdf

[17] Misiara, N., Alberi, A., Chauveau, A.-C., Chirpaz-Cerbat, D., Bourdelle, G., Desmons, M., France, A., Lacroix, M., Neyret, J., Leroy, P.-A., Perreu, G., Piquet, O., Pottin, B., Przybilski, H., Sellami, N.: Recent rf and mechanical developments for the ess rfq. In: Proc. LINAC'16, pp. 978–981. JACoW, Geneva, Switzerland, East Lansing, MI, USA (2016). https://proceedings.jacow.org/linac2016/papers/thplr054.pdf

[18] Zeng, R., Fedel, G.S., Jones, B., Miyamoto, R., Nicosia, D.J.P., Noll,

D., Sosa, A.G., Svensson, A.M., Trachanas, E., Baudrier, M., Chauveau, A.C., Desmons, M.J., Hamel, P., Piquet, O., Grespan, F.: Rfq performance during rf conditioning and beam commissioning at ess. In: Proc. LINAC'22, pp. 418–421. JACoW Publishing, Geneva, Switzerland, Liverpool, UK (2022). https://doi.org/10.18429/JACoW-LINAC2022-TUPOPA05 . https://proceedings.jacow.org/linac2022/papers/tupopa05.pdf

[19] Wangler, T.P.: RF Linear Accelerators, 2nd edn. Wiley-VCH, Weinheim (2008). https://doi.org/10.1002/9783527623426 . https://doi.org/10.1002/9783527623426

[20] Gad, A.F.: Pygad: An intuitive genetic algorithm python library. Multimedia Tools and Applications, 1–14 (2023)